

Stabilization of a passively mode-locked laser by continuous wave optical injection

Natalia Rebrova, Tatiana Habruseva, Guillaume Huyet, and Stephen P. Hegarty

Citation: *Appl. Phys. Lett.* **97**, 101105 (2010); doi: 10.1063/1.3483231

View online: <https://doi.org/10.1063/1.3483231>

View Table of Contents: <http://aip.scitation.org/toc/apl/97/10>

Published by the [American Institute of Physics](#)

Articles you may be interested in

[Optimum phase noise reduction and repetition rate tuning in quantum-dot mode-locked lasers](#)

Applied Physics Letters **104**, 021112 (2014); 10.1063/1.4861604

[Model for mode locking in quantum dot lasers](#)

Applied Physics Letters **88**, 201102 (2006); 10.1063/1.2203937

[Theory of mode locking with a fast saturable absorber](#)

Journal of Applied Physics **46**, 3049 (1975); 10.1063/1.321997

[rf linewidth reduction in a quantum dot passively mode-locked laser subject to external optical feedback](#)

Applied Physics Letters **96**, 051118 (2010); 10.1063/1.3299714

[Passive mode-locking in 1.3 \$\mu\text{m}\$ two-section InAs quantum dot lasers](#)

Applied Physics Letters **78**, 2825 (2001); 10.1063/1.1371244

[Distributed feedback gallium nitride nanowire lasers](#)

Applied Physics Letters **104**, 041107 (2014); 10.1063/1.4862193

AIP | Conference Proceedings

Get **30% off** all
print proceedings!

Enter Promotion Code **PDF30** at checkout



Stabilization of a passively mode-locked laser by continuous wave optical injection

Natalia Rebrova,^{a)} Tatiana Habruseva, Guillaume Huyet, and Stephen P. Hegarty
 Centre for Advanced Photonics and Process Analysis, Cork Institute of Technology
 and Tyndall National Institute, Lee Maltings, Cork, Ireland

(Received 30 March 2010; accepted 1 August 2010; published online 7 September 2010)

We investigate numerically and experimentally the properties of a passively mode locked quantum dot semiconductor laser under the influence of cw optical injection. We demonstrate that the waveform instability at high pumping for these devices can be overcome when one mode of the device is locked to the injected master laser and additionally show spectral narrowing and tunability. Experimental and numerical analyses demonstrate that the stable locking boundaries are similar to those obtained for optical injection in CW lasers. © 2010 American Institute of Physics. [doi:10.1063/1.3483231]

Quantum-dot (QD) mode-locked lasers (MLL) are excellent candidates for applications such as optical sampling, microwave photonics and optical time division multiplexed communication. Studies have indicated however that they are subject to a waveform instability that impacts negatively upon their time-bandwidth product (TBP).¹ This said, QD continuous-wave lasers have shown very stable optical injection locking characteristics, with no instabilities observed at zero detuning frequency over a wide range of master powers.² This observation then suggests that QD-MLL characteristics could be further improved and controlled through optical injection locking, for example for applications such as remote coherent receivers.³ This has previously been explored through the injection of two-tone coherent master light, which can be thought of as a form of optical injection in combination with hybrid modulation.⁴ In this paper we study the effect of single tone injection on QD-MLL performance both numerically and experimentally, where the laser mode-locking mechanism remains passive. Using the delay differential model described in⁵ with parameters derived from phase-sensitive pump-probe measurements we show that waveform instabilities can be suppressed by optical injection. We also present synchronization cones obtained by numerical tools as well as by experimental scanning.

We consider a model for a semiconductor mode-locked laser⁵ that has been applied to QD mode-locked lasers.⁶ The model expressed in dimensionless terms reads

$$\gamma^{-1}\dot{A} + A = \sqrt{\kappa}e^{(1-i\alpha_g)G_T - (1-i\alpha_q)Q_T/2}A(t-T), \quad (1)$$

$$\dot{G} = g_0 - \gamma_g G - e^{-Q}(e^G - 1)|A|^2, \quad (2)$$

$$\dot{Q} = q_0 - \gamma_q Q - s(1 - e^{-Q})|A|^2, \quad (3)$$

where A is an electric field envelope, G and Q are saturable gain and loss, respectively; T is the cold cavity round trip time; parameter γ represents the gain/losses bandwidth, κ is the attenuation factor describing linear non resonant intensity losses per cavity round trip, g_0 is pump parameter, which is proportional to the injection current in the gain region, $\gamma_{g,q}$ are the relaxation rates of the amplifying and absorbing sec-

tions, s is the ratio of the saturation intensities in gain and absorber media.

We numerically integrated equations for a laser with $T = 10$, $\gamma_g = 0.01$, $\gamma_q = 3$, $\kappa = 0.3$, $s = 30$, $\alpha_g = 2$, and $\alpha_q = 0.4$. This corresponds to a mode-locked laser with a 10 GHz repetition rate with an absorber recovery time of 13 ps and a gain recovery time of 100 ps as extracted from pump-probe spectroscopy measurements.^{7,8} We took $\gamma = 30$, which corresponds to a 17 nm gain bandwidth. For $q_0 = 3.5$, the mode-locking threshold occurs at $g_{0,th} = 0.11$ and a periodic pulse train is emitted [Fig. 1(b)] with an associated Lorentzian spectrum [Fig. 1(a)]. These pulses remain stable for $g_0 < 2.2g_{0,th}$ and become unstable for higher values of g_0 . In such a case [Figs. 1(c) and 1(d)], the optical spectrum broadens and a waveform instability appears.

Figure 2(a) shows three non-consecutive pulses (black, red, blue), offset for clarity and demonstrating the changing

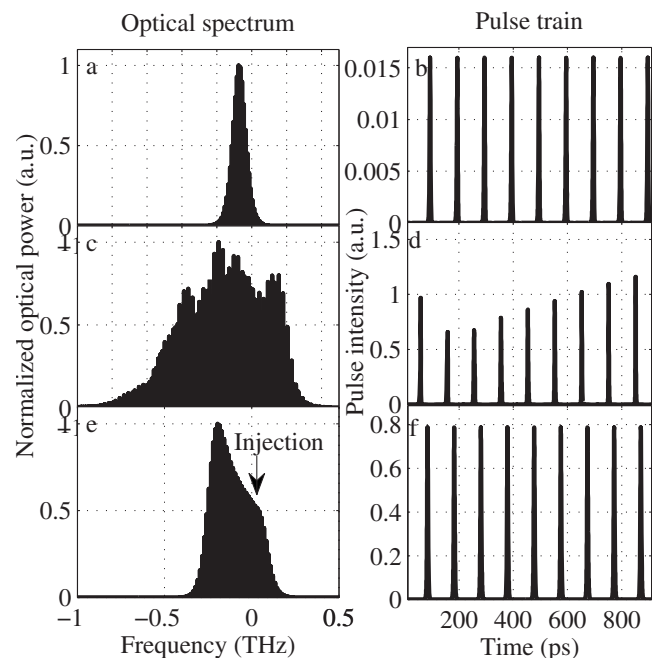


FIG. 1. Calculated pulses (b) and FTs (a) for free-running laser ($g_0 = 0.11$). Calculated pulses (d) and FTs (c) for free-running laser ($g_0 = 0.5$). Calculated pulses (f) and FTs (e) for injection locked laser ($g_0 = 0.5$).

^{a)}Electronic mail: nrebrova@gmail.com.

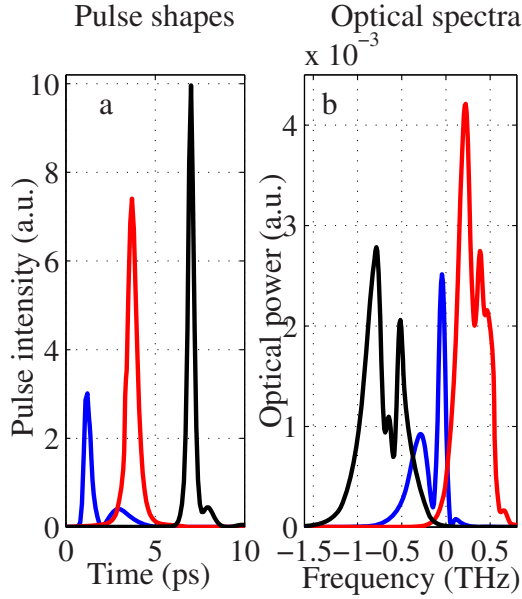


FIG. 2. (Color online) Calculated pulses (a) and FTs (b) for free-running laser ($g_0=0.5$).

pulse shapes. Calculated FTs of individual pulses are given in Fig. 2(b) (black, red, blue, plotted with 0.5 THz offset) differing from each other and from the spectral envelope calculated from a long pulse train Fig. 1(c).

To model optical injection we added a term $\eta e^{i\omega t}$ into Eq. (1), where η is the injection amplitude and ω is the detuning from the central frequency. With appropriate choice of η and ω we observed that injection suppressed the waveform instabilities which resulted in pulse stabilization and spectral narrowing, this is seen in Figs. 1(e) and 1(f) where the injected slave spectrum is shifted to the red side of the master wavelength. We found that this effect can be observed when using parameters $\alpha_g > \alpha_q$. Indeed, this condition and inequality $G - Q > \ln(\kappa)$ (which holds during the pulse) result in $\alpha_g G - \alpha_q Q > 0$, which causes the red frequency shift $-\Delta\omega = \alpha_g G - \alpha_q Q$, from the imaginary part of exponent in (1).

The experimental studies were carried out using uncoated two-section monolithic QD lasers emitting at 1.3 μm , with a repetition rate close to 10 GHz, and absorber section 12% of device length. An Agilent 8164B tunable laser source (TLS) with linewidth of 100 kHz was used as the master laser. The device was isolated from external reflections using polarization maintaining circulators and operated on a temperature controlled stage with 10 mK stability, an enclosure was used to shield the device and mount from air currents. The laser output was analyzed using a high-sensitivity autocorrelator, and under certain conditions the full electric field of the laser was reconstructed using a Southern Photonics EG130 frequency resolved Mach-Zehnder gate (FRMZG), more details of this instrument may be found in Ref. 9. From threshold (85 mA) to 1.4 times threshold (120 mA), the FRMZG reconstruction algorithm converged and the recovered pulse was confirmed by comparison with the laser optical spectrum and autocorrelation measurement. For currents above 1.4 threshold the FRMZG algorithm failed to recover physical pulse shapes, this is in accordance with previous work using a high-sensitivity frequency resolved optical gating (FROG) (Ref. 1) and is inter-

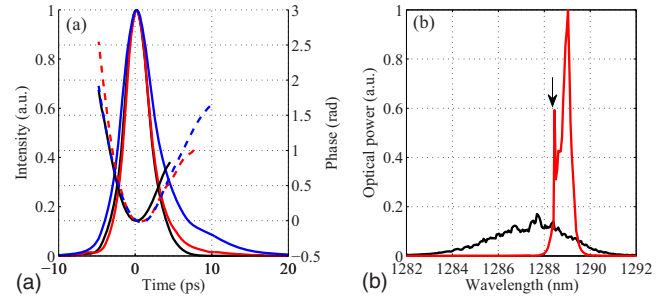


FIG. 3. (Color online) (a): Retrieved FRMZG pulses (solid lines) and phases (dotted lines) for 100 mA (narrowest), 120 mA (middle) and 130 mA (widest), absorber bias -6 V. (b) Optical spectra without injection (wide) and with injection (narrow).

preted as an outcome of waveform instability. With injection locking however, the FRMZG recovery always converged over the range of biases examined (up to 200 mA). The retrieved pulses demonstrated an asymmetrical pulse shape with faster leading edge and slower trailing edge and parabolic phase Fig. 3(a). For all injection wavelengths the slave laser mean wavelength was redshifted from the injection wavelength with the peak output shifted approximately 1 nm to the long wavelength side of the injection Fig. 3(b), this replicates the behavior observed in the numerical study, Fig. 1(e). Tuning of the slave spectrum over 8 nm via the master wavelength was also possible. These effects are highly similar to those noted for two-mode injection⁴ and the redshift phenomenon is understood as a consequence of unequal alpha-factors between the gain and absorber sections.

We measured the locking range by looking at the beating tone between the TLS and the nearest laser mode in the low frequency range. When the TLS wavelength was tuned closer to the laser mode the beating signal moved toward the zero frequency and disappeared when the laser locked. The beating tone appeared again at nonzero frequency when laser unlocked. The locking range obtained during experiments in two parameter space, injection power and master wavelength, is presented in Fig. 4, the slave power was 1 mW. Excessive master power led to stable single-mode emission, halting the mode-locking. It was observed during the experiment that the locking behavior was different on the upper

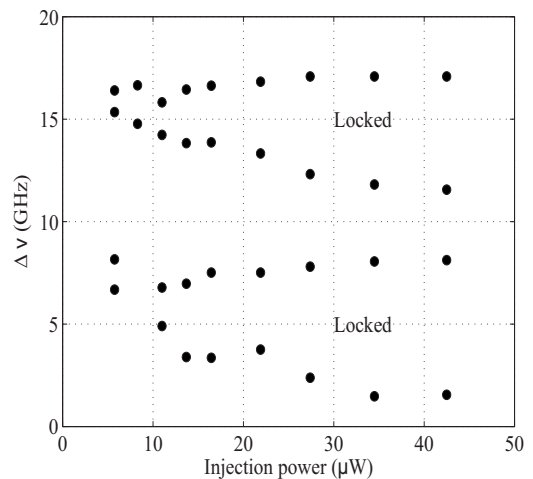


FIG. 4. Experimental synchronization cones. Slave power was 1.7 mW, $i=105$ mA, $V=-6.0$ V. Injection powers were estimated assuming a 50% coupling loss from the lensed fiber to the laser.

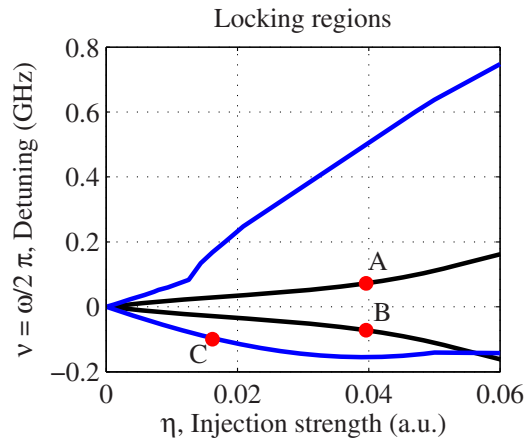


FIG. 5. (Color online) Theoretical locking regions for $\alpha_g=0, \alpha_q=0$ (black line) and for $\alpha_g=2, \alpha_q=0.4$ (blue line). $g_0=0.1$, $q_0=3.0$, $\kappa=0.3$, $s=30.0$, $\gamma=30.0$, $\gamma_g=0.01$, $\gamma_q=3.0$, $T=10$.

and lower boundaries of the synchronization cones.

The locking range of the locked state was also investigated using the DDEBIFTOOL (Ref. 9) package for Matlab. The black line on Fig. 5 bounds the locking region for $\alpha_g = \alpha_q = 0$. In this case the boundaries are symmetric with respect to central frequency. Points A and B denote bifurcations of codimension 2, i.e., at these points two pure imaginary and one real multipliers of the system cross the unit circle. For $\eta > 0.0396$ the loss of stability occurs via Hopf bifurcation and for $\eta < 0.0396$ periodic solutions of the system lose their stability via saddle-node bifurcation.

For $\alpha_g, \alpha_q \neq 0$ the optical spectrum of the laser is no longer centered on $\nu = \omega/2\pi = 0$ due to changes in refractive index. The vertex of the blue line on Fig. 5 which bounds the locking region for parameter choice $\alpha_g=2, \alpha_q=0.4$ was shifted for clarity by $\nu \approx 2.2$ GHz downwards. Moreover, the upper and lower boundaries are not symmetric in this case. The locking cone for the plotted range is bounded from below by saddle-node bifurcation alone and codimension point C on the upper boundary shifts to the left. Beyond C unequal alpha-factors for absorber and gain section lead to

different locking mechanisms on the upper and lower boundaries of the cone.

The increase of injection locking area with the inclusion of alpha, and its asymmetry, are well known phenomena in CW semiconductor slave lasers.¹⁰ In our case an equivalent of the analytical result of Petitbon *et al.*¹⁰ has not been shown, but work is on-going in this regard for a more limited parameter range.

In summary we have presented a theoretical and experimental study of the single mode injection effect on the performance of passively mode-locked QD lasers. We have demonstrated that the instabilities which occur for higher currents can be suppressed by locking to an external master laser which leads to decrease of the spectral width. We also obtained locking regions both numerically and experimentally.

The authors thank and acknowledge Andrei Vladimirov for invaluable discussions and advice.

This research was enabled by the Higher Education Authority Program for Research in Third Level Institutions (2007–2011) via the INSPIRE program and the authors also gratefully acknowledge the support of Science Foundation Ireland under Contract No. 07/IN. 1/1929.

¹Y.-C. Xin, D. J. Kane, and L. F. Lester, *Electron. Lett.* **44**, 1255 (2008).

²D. Goulding, S. P. Hegarty, O. Rasskazov, S. Melnik, M. Harnett, G. Greene, J. G. McInerney, D. Rachinskii, and G. Huyet, *Phys. Rev. Lett.* **98**, 153903 (2007).

³W. Lee and P. J. Delfyett, Jr., *Electron. Lett.* **40**, 1182 (2004).

⁴T. Habruseva, S. O'Donoghue, N. Rebrova, D. A. Reid, L. P. Barry, D. Rachinskii, G. Huyet, and S. P. Hegarty, *IEEE Photon. Technol. Lett.* **22**, 359 (2010).

⁵A. Vladimirov and D. Turaev, *Phys. Rev. A* **72**, 033808 (2005).

⁶N. Usechak, Y. C. Xin, C. Y. Lin, L. F. Lester, D. J. Kane, and V. Kovanis, *IEEE J. Sel. Top. Quantum Electron.* **15**, 653 (2009).

⁷I. O'Driscoll, T. Piwonski, C.-F. Schleussner, J. Houlihan, G. Huyet, and R. J. Manning, *Appl. Phys. Lett.* **91**, 071111 (2007).

⁸I. O'Driscoll, T. Piwonski, J. Houlihan, G. Huyet, R. J. Manning, and B. Corbett, *Appl. Phys. Lett.* **91**, 263506 (2007).

⁹K. Engelborghs, T. Luzyanina, and D. Roose, *ACM Trans. Math. Softw.* **28**, 1 (2002).

¹⁰I. Petitbon, P. Gallion, G. Debarge, and C. Chabran, *IEEE J. Quantum Electron.* **24**, 148 (1988).